Estimation of catchment-scale soil moisture patterns based on terrain data and sparse TDR measurements using a fuzzy c-means clustering approach

Ingmar Schröter*, Hendrik Paasche, Peter Dietrich, Ute Wollschläger

I. Schröter, H. Paasche, P. Dietrich, U. Wollschläger, Dept. Monitoring and Exploration Technologies, Helmholtz Centre for Environmental Research - UFZ, Permoserstraße 15, 04318 Leipzig, Germany; P. Dietrich, U. Wollschläger, WESS – Water and Earth System Sciences Competence Cluster, Keplerstraße 17, 72074 Tübingen, Germany; P. Dietrich, Centre for Applied Geoscience, University of Tübingen, Hölderlinstraße 12, 72074 Tübingen, Germany

*Corresponding author (ingmar.schroeter@ufz.de)

Contact details (*corresponding author):

Ingmar Schröter

Department Monitoring and Exploration Technologies

Helmholtz Centre for Environmental Research – UFZ

Permoserstraße 15, 04318 Leipzig – Germany

ingmar.schroeter@ufz.de

Tel. +49 341 235 1754

Fax +49 341 234 51939

Impact Statement

We present an efficient method for sampling and spatial estimation of soil moisture at the small catchment scale which is based on terrain data and sparse soil moisture measurements.

Abstract

Accurate characterization of spatial soil moisture patterns and their temporal dynamics is important to infer hydrological fluxes and flow pathways and to improve the description and prediction of hydrological models. Recent advances in ground-based and remote sensing technologies provide new opportunities for temporal information on soil moisture patterns. However, spatial monitoring of soil moisture at the small catchment scale (0.1-1 km^2) remains challenging and traditional *in situ* soil moisture measurements are still indispensable. This paper presents a strategic soil moisture sampling framework for a low-mountain catchment. The objectives were to: (i) find *a priori* a representative number of measurement locations, (ii) estimate the soil moisture pattern on the measurement date and (iii) to assess the relative importance of topography for explaining soil moisture pattern dynamics. The fuzzy c-means sampling and estimation approach (FCM SEA) was used to identify representative measurement locations for in-situ soil moisture measurements. The sampling was based on terrain attributes derived from a DEM. Five TDR measurement campaigns were conducted from April to October 2013. The TDR measurements were used to calibrate the FCM SEA to estimate the soil moisture pattern. For wet conditions the FCM SEA performed better than under intermediate conditions and was able to reproduce a substantial part of the soil moisture pattern. A temporal stability analysis shows a transition between states characterized by a re-organization of the soil moisture pattern. This indicates that, at the investigated site, under wet conditions topography is a major

control that drives water redistribution whereas for the intermediate state other factors become increasingly important.

Keywords: soil moisture, sampling design, cluster analysis, switching of states, pattern analysis

Introduction

Despite the importance of soil moisture patterns to derive information for hydrological, ecological, and pedological studies, spatial monitoring of soil moisture at the small catchment scale (0.1-1 km^2) remains a challenge. The interplay between static properties (e.g., topography, soil, geology) and dynamic processes (e.g., vegetation growth, evapotranspiration) is the reason why soil moisture is highly variable in space and time and the characterization of this variability is one of the major challenges within the hydrological sciences (Vereecken et al., 2014).

To observe the spatio-temporal dynamics of soil moisture at the small catchment scale, numerous measurement techniques are available including traditional *in situ* field measurements with various types of soil moisture sensors, geophysical measurement techniques, and passive and active microwave remote sensing (see e.g., Robinson et al., 2008; Wagner et al., 2007 for reviews). A drawback of the application of geophysical techniques is that the temporal resolution is often low and restricted to a few snapshots during the year and that the effectiveness of the different methods to spatially map soil moisture often depends on site conditions (e.g., soil texture, soil moisture state). Passive and active remote sensing data on airborne and space borne platforms have been widely used for detecting soil moisture at different wavelengths. However, at the small catchment scale remote sensing data are not yet operationally available to depict soil moisture patterns at adequate temporal and spatial resolution (Bronstert et al., 2012). For this reason, traditional *in situ* soil moisture measurements are still indispensable because they are straightforward in application and provide most accurate data. However, there is a trade-off between sampling density and spatial scale to observe soil moisture pattern dynamics by point measurements. Recent advances in sensing technology, in particular through wireless sensor networks (Cardell-Oliver et al., 2005; Bogena et al., 2010), allow for automated soil moisture monitoring in real time for the hillslope to the small catchment scale (Martini et al., 2015; Rosenbaum et al., 2012; (Penna et al., 2009; Bogena et al., 2010; Qu et al., 2015). However, these measurements are costly and hard to maintain, especially at agriculturally used sites. This is the reason why conventional soil moisture data collection is often done using portable sensors. Several studies collected *in situ* soil moisture on uniform grids or densely distributed and comprise hundreds of points for multiple sampling campaigns (Western and Grayson, 1998a; Wilson et al., 2003; Takagi and Lin, 2012; Hu and Si, 2014). Grayson et al. (1997) and Western et al. (1999a) demonstrated the use of "lots of points" (LOP) measurements (~500) to study the dynamics of spatial soil moisture patterns and their controls at the 10 ha Tarrawarra catchment in a temperate region in Australia. In their studies, they recognized that soil moisture patterns tend to switch between two preferred states depending on the seasonal evapotranspiration and precipitation ratio and the moisture state of the catchment. The observed patterns indicated a different degree of spatial organization (i.e., more organized for wet than dry state) related to the dominant hydrological process controlling the soil moisture distribution. The dry state is dominated by vertical fluxes, with local controls including soil properties and local terrain (areas of high convergence) shaping the spatial pattern. The wet state is dominated by lateral water movement through both surface and subsurface paths, with nonlocal controls which represent the dominant influence of catchment terrain on the distribution of soil moisture. Merz and Plate (1997) showed that organization in spatial patterns of soil moisture at particular times and soil properties may have a dominant influence on catchment runoff. Moreover, Western and Grayson (2000) demonstrated the use of observed patterns to improve the development, calibration and testing of a distributed model.

Systematic comprehensive observation campaigns like the ones of the Tarrawarra study (Western et al., 1999b) or the Mahurangi catchment (Woods et al., 2001) are rare because they are labor intensive and time consuming. Therefore, there is a need for new measurement designs which are technically and economically feasible, while maximizing information content (Soulsby et al., 2008). The challenging questions to design such strategic sampling schemes for *in situ* soil moisture measurements include: (i) how to define *a priori* an appropriate number of representative measurement locations?, and (ii) how to regionally estimate soil moisture patterns (from point observations) for a target area by using sparse *in situ* measurements and readily available ancillary data so that the derived spatial information matches the model resolution or the footprint of high-resolution remote sensing data to which it is being compared?

Vachaud et al. (1985) were the first who introduced the concept of temporal stability (TS) in soil moisture monitoring to reduce the measurement effort to characterize the spatial soil moisture pattern of large fields. TS is described as the temporal persistence of a spatial pattern which implies that particular locations exist in the field that always display mean behavior while others are persistently wet or dry (Kachanoski and de Jong, 1988). Currently, the number of publications on TS of soil moisture is growing quickly mainly in applying the TS concept to select one or more locations out of a larger sampling volume to estimate average soil moisture for the field to catchment scale (Grayson and Western, 1998; Martínez-Fernández and Ceballos, 2005; Martinez et al., 2008; Schneider et al., 2008; Zucco et al., 2014). However, such a catchment average soil moisture monitoring (CASMM), introduced by Grayson and Western

(1998), does not aim to describe the spatial patterns (e.g., zones of saturation), relevant for the movement of water, and to shed light on the reason for TS and its controls. Therefore, other sampling techniques are needed that use available knowledge about structure forming processes allocated to disciplines of pedology, biology, hydrology, and geomorphology, to expand sparse measurements to a continuous representation of the soil moisture pattern (Schulz et al., 2006). Recently, this approach has shaped the field of hydropedology (Lin, 2003) that uses pedometrics to study the spatial patterns of soil properties and the related temporal dynamics of water in the vadose zone. In this framework, various sampling techniques have been proposed and tested to efficiently capture catchment/environmental conditions. These include stratified random sampling (SRS) (McKenzie and Ryan, 1999; De Gruijter et al., 2006), response surface sampling (RSS) (Lesch, 2005) or conditioned Latin hypercube sampling (cLHS) (Minasny and McBratney, 2006; Schmidt et al., 2014), to name a few, to find sampling locations assisted and guided by the presence of ancillary data, such as terrain attributes, geophysical measurements, remote sensing images or vegetation maps. The sampling points are then chosen to optimize the soil property/ancillary data relationship. Furthermore, Werbylo and Niemann (2014) tested the effectiveness of SRS and cLHS to select a limited number of points for soil moisture monitoring based on topographic data and to calibrate two different models to estimate soil moisture patterns at three catchments.

To find representative sampling locations for soil moisture measurements *a priori* knowledge of key drivers of soil moisture patterns is essential. The general idea behind this is based on the soil-landscape paradigm proposed by Jenny (1941) which was further generalized and formulated by McBratney et al. (2003). In short, the spatial variability of a soil attribute is the result of spatially referenced soil forming factors (environmental covariates) which can be used to establish soil spatial prediction functions (McBratney et al., 2003). Considering soil moisture as a dynamic soil attribute, a general prediction model can be described as

$$\theta(x, y, z, t) = f(Q) \quad [1]$$

where Q is a set of p environmental variables (i.e., surrogate patterns) that provide information about the underlying catchment characteristics. They can, for example, be derived from GIS, proximal soil sensing, and remote sensing. $\theta(x,y,z,t)$ stands for the soil moisture at some spatial location $x,y,(z)$ at time t. The general problem consists in the definition of zones (clusters) with similar environmental characteristics which are assumed to show similar hydrological response (i.e., soil moisture dynamics). In each zone, a soil moisture monitoring location and a set of collocated environmental variables exist to build a function f which is flexible enough to describe a nonlinear relationship. Based on this empirical quantitative function, spatial estimates are made from observation data to infer soil moisture at unsampled locations. To follow this approach a main task is the identification of representative zones and to derive the soil-landscape relationships. With the advent of pattern recognition in the late 1960s the usage of the fuzzy clustering technique has continuously found its way into geosciences. Since then, fuzzy classification has been applied in many fields to extract knowledge based on ancillary data for automated landform classification (Burrough et al., 2000; MacMillan et al., 2000) and soil classification (Odeh et al., 1992; Triantafilis et al., 2013). However, the performance of the fuzzy clustering also depends on the considered set of factors and is sensitive to the selected number of clusters (Stevenson et al., 2015; Sun et al., 2012). Fuzzy classes have also been used to identify sampling locations for mapping soil types (Odeh et al., 1990) and soil moisture (Van Arkel and Kaleita, 2014). Furthermore, the study of Schmidt et al., (2014) where a fuzzy sampling scheme was compared to other sampling schemes supports the usefulness of this method in combination with nonlinear multiple regression (i.e. random forest) to predict soil properties at the field-scale.

The general advantage of the fuzzy classification method is that it allows for class overlap to account for gradual transitions which often occur in the environment (Burrough et al., 2000). The objectives of this study are to apply a strategic sampling design based on a fuzzy c-means clustering technique (Paasche et al., 2006) to identify *a priori* a limited number of representative sampling locations to monitor near-surface soil moisture dynamics at the small catchment scale, (ii) to apply the sampling framework to spatially estimate soil moisture pattern on the measurement date, and (iii) to assess the relative importance of topography for explaining soil moisture pattern dynamics at the small catchment scale for the catchment under investigation.

Theoretical background of the FCM sampling and estimation approach (FCM SEA)

Fuzzy c-means clustering technique

The fuzzy c-means (FCM) clustering technique can be applied to stratify a catchment, based on a set of environmental covariates (i.e., proxies for soil moisture controlling factors), into a specified number of clusters. In this paper, we call these clusters soil landscape descriptors (SLDs) where it is expected that samples belonging to each SLD show similar soil moisture response. The geospatial data of the catchment are arranged in a $n \times p$ matrix $\mathbf{X}$, with element x_{ik}, n is the number of data points (pixels) and p is the number of predictor variables (e.g., environmental variables such as terrain attributes) with $i = 1 \dots n$ and $k = 1 \dots p$. The optimal classification for a selected number of c clusters is iteratively found so that the multivariate within-cluster variance is as small as possible (Burrough et al., 2000). This is obtained by minimizing the following objective function (Bezdek, 1974):

$$J_{FCM} = \sum_{i=1}^{n} \sum_{j=1}^{c} m_{ij}^{\phi} \left(D_{ij}\right)^2 \text{, where} \qquad [2]$$

m_{ij} denotes the degree of membership of a data point to a distinct cluster and D_{ij} is a selected distance measure, defined here as Euclidean: ${D_{ij}}^2 = \left\|\mathbf{x}_i - \mathbf{v}_j\right\|^2$.

After selecting the number of clusters and minimizing the objective function (Eq. 2), the final outcome of the FCM clustering provides a fuzzy membership matrix **M** with elements m_{ij} and a matrix of cluster centers **V** with elements v_{jk}. In fuzzy logic, each element is assigned a partial membership to all clusters based on their distance to the respective cluster center. The membership values vary between zero and one; the the value the closer the element is to the corresponding cluster center. The exponent ϕ determines the degree of fuzziness. For ϕ approaching one, the algorithm resembles a crisp classification algorithm that only allows an individual pixel/data point to lie in one mutually exclusive cluster , while for larger values it allows an individual to be partial member of all clusters (i.e., the membership to a specific cluster is more fuzzy). In our study, ϕ was set to 1.6, which is widely accepted as suitable choice in literature (Bezdek et al., 1984). The membership m_{ij} of the *i*th object to the *j*th cluster is determined by

$$m_{ij} = \frac{D_{ij}^{-2/(\phi-1)}}{\sum_{l=1}^{c} D_{il}^{-2/(\phi-1)}}, \qquad [3]$$

where the sum of all membership values of an element across all clusters is unity. The cluster center v_{jk} of the *j*th cluster for the *k*th attribute is calculated as

$$v_{jk} = \frac{\sum_{i=1}^{n} (m_{ij})^{\phi} x_{ik}}{\sum_{i=1}^{n} (m_{ij})^{\phi}}. \qquad [4]$$

One important issue in all clustering techniques is the choice of an appropriate number of clusters which is inherently subjective. This is known as “cluster validity problem” which strives to offer a quantitative (statistical) measure which indicates how well the algorithm has identified the structure that is present in the underlying ancillary data. Therefore, many authors have proposed validity functionals in order to solve the validity problem. The fuzzy performance index (FPI) and the normalized classification entropy (NCE) are two of these functionals which were found to be most useful (Roubens, 1982) and are widely used in literature (Burrough et al., 2000; Triantafilis et al., 2003). The FPI is a measure of the degree of fuzziness and the NCE indicates the degree of disorganization in the classification. The least fuzzy and disorganized number of clusters is considered optimal (Odeh et al., 1990). After finding the optimal number of clusters, defuzzification techniques (Leekwijck and Kerre, 1999) are used to define crisp classes in order to perform a geoscientific interpretation of every class. The general workflow of this approach has been used by others (e.g., Paasche and Eberle, 2009) and is displayed in Figure 1.

Our proposed method is based on the work of Paasche et al. (2006) but works in a modified way (Fig. 2) because the purpose of our sampling strategy is to identify locations that represent the range of values of each ancillary variable so that the sampling is less likely to be redundant. Therefore, we consider the FCM clustering as imaging technique using the membership matrix **M** and the center matrix **V** to store the spatial heterogeneity and average cluster-specific information, respectively. These elements are of central importance because they describe the complex landscape structure in a reduced form. Using a simple mixing law, the ancillary data can be reconstructed from the membership and center matrices (Fig. 2).

The reconstructed maps are stored in a matrix **B** and the reconstructed value of the *i*th data point for the *k*th attribute is calculated as a weighted sum over all clusters:

$$b_{ik} = \sum_{j=1}^{c} m_{ij}\, v_{jk}. \qquad [5]$$

Comparing the reconstructed and the attribute data allows the quantification of informational loss during the clustering procedure. To account for this the total absolute difference (TAD) was calculated:

$$TAD = \sum_{i=1}^{n} |\mathbf{b}_i - \mathbf{x}_i| \quad [6]$$

where $\mathbf{b}_i$ and $\mathbf{x}_i$ are reconstructed and attribute data points.

A simple L-curve analysis (e.g., Twarakavi et al., 2010) of informational loss over different numbers of clusters allows for the identification of an optimal number of clusters. L-curve analysis is a well-established technique to identify the optimal regularization strength for ill-posed discrete optimization techniques (e.g., Lassonde, 2001) which constrains the spatial/structural complexity of the final solution. In our case, the number of clusters constrains the complexity of the solution of the cluster analysis and thus the ability to capture the spatial heterogeneity of all considered ancillary data in the fuzzy membership matrix. The selection of an optimal number of clusters ensures that sufficient information is stored in the membership matrix **M** to reconstruct the complex patterns/structures of the ancillary data. In case the "elbow" point cannot be detected uniquely by visual inspection it is advisable to better increase the number of clusters towards a very conservative optimal number of clusters to avoid the risk of losing structural information and we have followed this strategy in this study. Figure 3 conceptually shows the TAD relationship for different cluster solutions and the "elbow" point where the information loss saturates. The fuzzy membership matrix of this optimal solution (c_{opt}) is then further analyzed for the identification of suitable sampling locations (e.g., Hachmöller and Paasche, 2013). Note, for the case of noise-free ancillary data, one could rank the sampling locations according to the values of maximal membership to a cluster. For example, the point, where maximal membership to a cluster is achieved would be the most appropriate one for soil moisture sampling. However, the ancillary data are not free of noise components which are not specifically known for every data point. According to the principles of error propagation, this noise will propagate into the membership values not allowing for a strict ranking of optimal sampling locations. Thus, we are only searching for a point with high membership value to a cluster but not for the point with highest membership. Practically, this makes our approach very applicable to regions of rough and hardly or inaccessible terrain, since the condition to sample a very specific point in the study region is not restricted to a single sampling location but rather to a subset of points. Therefore, the memberships of c_{opt} are used to identify areas within the zones which have at least a membership of 0.8 to a corresponding class. For each class a minimum of one location is selected to form a sparse set of sampling points.

Estimation of soil moisture patterns

Following Paasche et al. (2006) and (Hachmöller and Paasche, 2013) we use sparse measurements and the fuzzy membership matrix describing the spatial heterogeneity of the attributes to estimate soil moisture spatial patterns . This is done by calibrating each cluster with a point soil moisture measurement thus extending the center matrix **V** achieved by clustering the ancillary/physiographic data sets. This extension is done by adding a column to the matrix containing the measured soil moisture value for each cluster obtained from the sampling locations derived with the FCM clustering. Taking the fuzzy membership matrix as spatial weighting information (equation 5) for the soil moisture information stored in the extended center matrix **A** we achieve a spatially continuous prediction of soil moisture distribution (Fig.2). This approach holds if the variable of interest is related to at least one of the underlying physiographic attributes influencing the pattern in the fuzzy membership matrix. Prediction is done without knowing or specifying the exact relation of the target value (i.e., soil moisture) to any of the underlying ancillary data. However, since only structural heterogeneity described by the membership values is used to guide the prediction of the spatial distribution of the target value, this approach will likely fail, if the ancillary database does not reflect the various dependencies of the target value.

Site Description

The Schäfertal research site (11°03′E, 51°39′N) is a small low-mountain catchment and is part of the long-term Earth observation network TERENO (Zacharias et al., 2011). It is located on a plain in the Lower Harz Mountains in central Germany, approximately 150 km southwest of Berlin (Fig. 4). The Schäfertal catchment has a humid continental climate and the mean annual air temperature is 6.8 °C ranging from -1.8 °C in January to 15.5 °C in July (Ollesch et al., 2006). Mean annual precipitation is about 630 mm (time series 1968-2006) which is low compared to other low mountain-areas in Germany due to the leeward position of the region on the eastern slope of the Harz Mountains (Reinstorf, 2010). From April to September, the climatic water balance yield according to the closest weather station, 9 km away, in Harzgerode, is negative (-64 mm) whereas the long-term mean of the annual climatic water balance is +126 mm (Abdank et al., 1995).

The size of the agriculturally used catchment is 144 ha. Its elevation ranges from 393 m a.s.l. from the outlet of the catchment to 445 m a.s.l. on the highest ridge. The catchment is V-shaped with a first order stream in the valley and with gentle to moderate slopes (up to 20%) on both sides of the stream. The site is characterized by four distinct landforms: 1) north-facing slope, 2) south-facing slope, both intensively used for agriculture, 3) valley bottom with pasture or meadow and 4) topographic depressional areas (swales) disrupting the slopes on both sides of the stream. In autumn 2012, parts of the grassland area in the western part of the catchment were transformed into arable land.

The catchment is underlain by Devonian greywacke and shale which are covered by a complex of periglacial layers with different fractions of silt and rock fragments (Altermann, 1985). Different soils evolved according to the sequence of the cover layer and landscape position. The dominant soils comprise Luvisols and Cambisols on the hillslopes and peaty Gleysols in the valley bottom (Borchardt, 1982).

Material and Methods

Selection of ancillary data

To capture the spatio-temporal variability of soil moisture in the Schäfertal catchment the sampling needs to be driven based on the digital implementation of external drivers of soil formation that control processes of water redistribution. Therefore, the selection of appropriate ancillary data requires understanding of the physical significance of patterns of specific environmental variables to provide information which is in some way related to soil moisture (Grayson et al., 2002). We follow a very simple approach and use topographic information for this purpose. Recalling the soil-landscape paradigm (Hudson, 1992), topography at the small catchment scale is an integral factor that has a lasting influence on the effects of gravitation, water, biota, microclimate and soil formation and is therefore one of the most widely used static factors that affects runoff processes (Western et al., 1999a; Beaudette et al., 2013). Of course there is no reason per se to expect that topography solely explains soil moisture variability. Previous studies show that in some settings the use of terrain indices perform well, while in other settings they have been shown to perform poorly (Western et al., 2004). So we are well aware that topography is not the only factor controlling soil moisture pattern dynamics but we can test how much of the soil moisture pattern can be described in our research catchment by following this rather simple approach. To this end, we used a digital elevation model (DEM) to derive terrain attributes that may be related to key hydrological processes controlling the spatial distribution of soil moisture in the Schäfertal catchment.

Digital Terrain Modelling

Terrain information was obtained from a high-resolution 1×1 m^2 digital elevation model (DEM1) derived from an airborne laser scanning (LIDAR) of the Schäfertal catchment (GeoBasis-DE / LVermGeo LSA, 2009). Such a high resolution DEM was used to describe the spatial arrangement of topographic structures (e.g., swales) in detail as they are relevant for soil moisture redistribution and to approximate the sampling support for soil moisture measurements. To reduce the amount of noise in the LIDAR data and to better represent primary topographic attributes within the catchment, a 10×10 m^2 filter window was applied to the original DEM using ArcGIS 10.1 (ESRI, Redland, CA). By choosing this filter window, we calculated the mean elevation of all cells within the window and applied the mean value to the corresponding center cell. For practical reasons, the smoothed DEM was additionally resampled into a 2×2 m^2 DEM (DEM2) with bilinear interpolation. For hydropedological applications, a wide range of terrain attributes are available that describe relevant features in the catchment with respect to soil moisture redistribution (Moore et al., 1991; Behrens et al., 2010) and we assume that they are useful for the identification of representative monitoring locations. We derived four topographic attributes: slope, elevation, total annual incoming solar radiation (TIR) and SAGA wetness index (SWI). Each attribute independently contributes information about local and contextual landscape conditions and is commonly used in the literature (Western et al., 1999a; Wilson et al., 2005;

Takagi and Lin, 2012). By this means, the elevation was used to describe landscape position and the gravitational potential energy that drives water flow. The slope is indicative to represent the hydraulic gradient that drives surface and near-subsurface fluxes (Western et al., 1999a). The TIR was used as an index for evapotranspiration and microclimate and the SWI to represent zones of surface saturation. Note that we used SWI instead of topographic wetness index (TWI) as introduced by Beven and Kirkby (1979). The SWI is a modified version of the TWI to account for a more realistic prediction for cells situated in valley floors with small vertical distance to a channel (Böhner and Selige, 2006). All terrain attributes were calculated with SAGA-GIS (System for Automated Geoscientific Analyses) (see Wilson and Gallant (2000) for algorithms). These computations yielded gridded data sets of 4 attributes (Fig. 5a-d) with a spatial resolution of 2 m and form the input data for the fuzzy c-means cluster algorithm.

Selection of Sampling Locations for Estimation of Soil Moisture Patterns

The FCM clustering was conducted separately for the arable land and for the grassland. We derived 20 clusters for arable land and 10 clusters for grassland, respectively. Figure 6 shows the distribution of clusters with the clusters for both land uses being merged in one map. Taken together, they form the 30 SLDs for the Schäfertal catchment. Then, each cluster was assigned with at least one "sparse" measurement point. In this study, we determined altogether 50 measurement points for TDR by placing two measurement points in each cluster on the arable land (hillslope areas) and one in each grassland cluster (riparian zone). The two measurement locations for the arable land were chosen as the total area is much larger than that of grassland and this way to account for within cluster variation and to avoid local extrema which would influence the interpolation. For a catchment area of ~1.5 km^2 a number of 50 measurement points is "sparse" in the sense that this number would be way too small for an interpolation of soil moisture maps based on geostatistical approaches such as kriging. Nevertheless, conducting the analysis with 30 measurement points (one per cluster) would also be feasible.

For validation of the soil moisture maps, we used an independent set of 44 TDR measurement points distributed all over the catchment. Thirty of these locations were obtained from simple random sampling across the whole catchment and 14 points were available from a Latin hypercube sampling which was available from an already running time series of measurement campaigns and was designed to provide local ground truth (soil moisture and vegetation parameters) for remote sensing measurements. However, all these measurement points were independent from the locations determined for the FCM sampling.

In combination with the calibration points a total of 94 monitoring locations were determined for the catchment (Fig. 7), which lead to a measurement effort of a half day work. Each sampling point was georeferenced with a Leica GPS1200 (Leica, Heerbrugg, Switzerland) with a lateral and vertical resolution of 0.1 m, and the locations were marked. The near-surface (0-10 cm) volumetric soil moisture was sampled using a portable TDR100 time domain reflectometer (TDR) (Campbell Scientific, Logan, UT) with a custom-made three-rod probe, with a basic accuracy of $\pm$ 0.02 m^3/m^3. Before measuring, TDR probes were calibrated for soil moisture estimation with measurements in water and air. Volumetric soil moisture θ [m^3/m^3] was calculated using the CRIM (Complex Refractive Index Model) formula according to Roth et al. (1990). Furthermore, soil temperature was measured with a DT-300 handheld LCD-thermometer (Voltcraft, Hirschau, Germany), with a basic accuracy of $\pm$ 1 °C, in 3-6 cm depth. The temperature data were used for temperature correction of the dielectric permittivity of water ε_w. The dielectric permittivity of the soil matrix ε_s was set to an estimated value of 4.6 [-]. The porosity of the soil was estimated based on soil information data (Borchardt, 1982) and was set to

0.4 for Cambisols and Luvisols on the slopes, and to 0.6 and 0.75, respectively, for the Gleysols in the lower relief positions near the channel and for the peat soils. At each point, campaign-based TDR measurements were conducted to acquire local soil moisture contents based on the average of three replicate TDR measurements.

Soil Moisture Measurement Campaigns and Timing

From spring to autumn 2013 five measurements campaigns (T1 to T5) were conducted in the Schäfertal catchment. The timing of the five field campaigns was designed to capture a range of soil moisture states. The moisture contents covered a wet (April-May 2013) moisture state due to the late snow melt in 2013 and an intermediate (September-October 2013) soil moisture state typical for fall conditions in the Lower Harz Mountains. A dry state could not be captured for the entire catchment due to limited access to the cropped fields during the summer.

All points were measured within a few hours (< 6h) to minimize the effect of evapotranspiration and drainage processes on the soil moisture measurements. The measurement campaigns were further optimized by calculating the shortest route for visiting each point with the Concorde Travelling Salesman (TSP) Solver (Applegate et al., 2001, see www.math.uwaterloo.ca/tsp/concorde/).

The temporal persistence of soil moisture patterns was tested by calculating the non-parametric Spearman rank correlation coefficient r_s for the various sampling dates (Vachaud et al., 1985). The Spearman rank correlation coefficient for soil moisture values measured at observation times u_1 and u_2 is computed as

$$r_s = 1 - \frac{6\sum_{i=1}^{n}\left(R_{i,u_1} - R_{i,u_2}\right)^2}{n(n^2-1)} \qquad [7]$$

where n is the number of point soil moisture observations in the catchment, R_{ij} is the rank of θ_{ij} at location i at observation time u. The closer r_s is to unity, the more temporally stable are the patterns. In this respect, our intention to apply this coefficient is to check for temporal changes in soil moisture spatial organization which would not be explainable by the static topographic data used in our FCM clustering procedure.

FCM validation and estimation error

To assess the prediction accuracy of this nonlinear estimation technique we calculated the Nash–Sutcliffe coefficient of efficiency (NSE) (Nash and Sutcliffe, 1970) and the root mean square error (RMSE). Therefore, the independent validation data set composed of 44 soil moisture observation points over the whole catchment was used. The NSE was used to explain how well the model matches the observed soil moisture pattern. The RMSE indicates the accuracy of the model to match the observed soil moisture. The NSE is defined as

$$NSE = 1 - \frac{\sum_{t=1}^{a}\left(\theta_t - \hat{\theta}_t\right)^2}{\sum_{t=1}^{a}\left(\theta_t - \bar{\theta}\right)^2} \qquad [8]$$

where a is the number of data points in the validation data set, θ_t is the tth observed soil moisture, $\hat{\theta}_t$ is the predicted soil moisture of the tth observation and $\bar{\theta}$ is the average of the observations. The RMSE is determined by

$$RMSE = \left(\frac{1}{a}\sum_{t=1}^{a}\left(\theta_t - \hat{\theta}_t\right)^2\right)^{1/2}. \qquad [9]$$

The statistic software R (R Development Core Team, 2012) and the R package e1071 version 1.6-1 (Meyer et al., 2014) was used to carry out the FCM clustering and to perform all statistical analyses.

Results

Soil moisture measurements

The main statistics of the five selected TDR sampling campaigns are provided in Table 1. The first TDR campaign was conducted on April 17, 2013 right after the snowmelt, and was followed by a second campaign on April 23, 2013 after one week of drying, and a third one on May 8, 2013 three weeks later with a small amount of rain between the second and the third campaign. The fourth campaign was conducted on September 25, 2013 followed by the fifth measurement on October 2, 2013 after one week of drying. T1 to T3 represent a wet moisture state and show high spatial mean soil moisture values (0.34, 0.26, and 0.27 m^3/m^3, respectively) throughout the catchment whereas T4 and T5 represent an intermediate state with moderate spatial mean soil moisture values (0.19 and 0.18 m^3/m^3, respectively). The spatial patterns of the five TDR measurement campaigns are displayed in Fig. 8.

All five measurement dates show a valley-dependent pattern of soil moisture with higher values occurring in the valley bottom. However, the pattern for the wet moisture states (T1 to T3) is more pronounced with higher ranges between 0.49 to 0.55 m^3/m^3 and higher standard deviations from 0.09 to 0.11 m^3/m^3 for soil moisture contents (Tab. 1). The very high moisture contents in the valley bottom (> 0.5 m^3/m^3) highlight locations with a peaty soil layer and high porosities at the top of the soil profile that are in strong contrast to the soil moisture of the mineral soils with lower porosities which, however are also at or close to saturation right after the snowmelt (0.3 to 0.4 m^3/m^3) (Fig. 8a-7c). Moreover, soil moisture values are higher on the north-exposed slope than on the south-exposed slope which cannot be explained by topography only and which is also contradictory to what would be expected from atmospheric forcing. The pattern for the intermediate state (8d-8e) is less prominent with smaller soil moisture ranges between 0.36 and 0.37 m^3/m^3 (Tab. 1) than the one observed during the wet state that displays strong alignment along the valley and converging hillslopes.

Estimated soil moisture patterns

Figure 9 shows the soil moisture patterns for all five sampling campaigns estimated for the entire catchment area with the FCM clustering approach using 50 TDR measurement points for calibration based on the topography-based sampling scheme (Fig. 2).

All estimated patterns show the topographic dependence of soil moisture with increasingly wet areas in the depression lines (swales) and in the valley bottom. For the measurement dates T1 to T3 (Fig. 9a–9c) they also indicate the difference in soil moisture between the northern and the southern hillslope with higher soil moisture contents predicted for the northern slope. To test how well topography is suited to reproduce the observed soil moisture patterns, the prediction accuracy was estimated using the Nash-Sutcliffe Coefficient of Efficiency (NSE) based on the measurements at the 44 validation points. The predicted and observed soil moisture values for the five measurement dates are displayed in Figure 10. In addition to that, Table 3 shows the performance when the validation is separately conducted for arable land and grassland (riparian zone) and for the whole catchment. For the measurement dates T1 to T3 during the wet state, the FCM SEA performs well for the whole catchment and shows high NSE values (T1: 0.78; T2: 0.73; T3: 0.59) (Fig. 10). In contrast, the FCM performance is weaker during intermediate soil moisture states on dates T4 and T5 (T4: 0.34; T5: 0.41). The RMSE for the whole catchment yielded for all five sampling dates similar results with moderate accuracy (0.05–0.06 m^3/m^3). However, there is a strong contrast in the performance between the two land use types. For arable land the estimates are almost always more accurate than for grassland with much smaller RMSE

(Table 3). For the wet state, T1 to T3, arable land outperforms grassland and shows more consistent NSE values than grassland. For the intermediate state, T4 to T5, the performance for both land use types decreases and shows negative NSE values for grassland and a negative and a positive NSE value for arable land. Note that negative NSE values indicate that the observed average soil moisture is a better estimate of the observed pattern than the estimated pattern obtained with the FCM SEA.

Temporal stability of soil moisture patterns

Table 2 provides an overview of the Spearman rank correlation coefficients calculated for all measurement dates. For the wet soil moisture state (T1 to T3) the spatial patterns show a high rank correlation ($r_S \geq 0.87$) indicating that the patterns are very similar during this time. Comparison of the moisture patterns of the wet state (T1 to T3) with the intermediate state (T4 and T5) results in significantly lower rank correlations ($r_S \leq 0.66$), while the moisture patterns during the intermediate states exhibit again a higher rank correlation ($r_S = 0.79$). This analysis shows that the soil moisture patterns in the Schäfertal reorganize from the wet to the intermediate state.

Discussion

Controls of spatio-temporal organization of soil moisture for the wet and intermediate states

For the Schäfertal catchment, the performance of the FCM SEA decreases as the catchment becomes drier (Fig. 10). Moreover, there is significant shift in NSE values between the wet and the intermediate soil moisture conditions, indicating that the relative importance of topography diminishes and the relative importance of factors such as soil heterogeneity (i.e., texture, structure) and vegetation (i.e., crop type, land use, density) become increasingly important and drive soil moisture variation. Additionally, we attribute the shift to the fact that evapotranspiration is the controlling factor fostering vertical flow processes within the soil profile during the summer and fall months. This would also support the work of Albertson and Montaldo (2003) who provided a theoretical framework that demonstrated that vegetation can reduce soil moisture spatial variability as soon as a positive covariance between transpiration and the soil moisture field emerges. Since the estimated spatial pattern described from the fuzzy membership information relies on topographical attributes only we are not able to reproduce this pattern re-organization.

For the wet state, the FCM SEA based on a combination of single terrain attributes already explained between 59% and 78% of soil moisture variability. The predicted patterns of soil moisture (Fig. 9) reflect the terrain features well showing high soil moisture in the riparian zone (valley) and converging areas (swales/hollows). Our findings correspond well to the hydrotope map of the Schäfertal (Borchardt, 1982) that indicates a shallow groundwater table close to the surface in the central part of riparian zone and in the converging areas. Additionally, field observation shows failed sprouting due to waterlogging with the beginning of the growing season in the converging areas. For this reason, there is evidence that the estimated maps produce a realistic pattern under wet conditions and thus topography is an important control for soil moisture patterns during these times in the Schäfertal catchment.

For dryer states our proposed terrain-driven sampling and estimation approach performs less accurate but is still capable of explaining between 34% and 41% of total variance. This is still relatively good compared to most other studies which rarely explained more than 50% of soil moisture variability using topographic data (Western et al., 1999a; Takagi and Lin, 2012; Wilson et al., 2005; Beaudette et al., 2013). However, for both moisture states the accuracy of the estimated soil moisture is moderate with an average RMSE of 0.06 m^3/m^3. Our proposed FCM SEA showed seasonality in the prediction accuracy that is in line with the studies that used terrain indices to explain soil moisture variability. However, it should be noted that at our site, the FCM SEA performance is better and more accurate (small RMSE) for arable land than for the grassland areas in the valley bottom (Fig. 10, Table 3). We presume that this is due to the fact that topography is less prominent in the riparian zone and expect other factors such as groundwater influence and soil properties to be more important. Moreover, these areas show also small-scale variability in soil moisture due to microtopography which is caused by hummocks and depressions of the grassland patches which is not captured by the DEM.

Our temporal stability analysis on the observed soil moisture patterns provides an additional explanation for the seasonality in the prediction accuracy of the FCM SEA. The analysis shows that temporal re-organization of the soil moisture spatial pattern occurs during the year in the Schäfertal catchment. There is at least a transition from a highly organized pattern during wet conditions towards a more uniform distribution under intermediate conditions. Previous studies that examined seasonal changes in near-surface soil moisture spatial organization attributed the reorganization of soil moisture patterns to variable rates of evapotranspiration and root water uptake by plants (Hupet and Vanclooster, 2002; Baroni et al., 2013), a change from predominantly lateral soil water movement to predominantly vertical soil water movement (Grayson et al., 1997; Western et al., 1999a), or to simply soil textural differences (Famiglietti et al., 1998).

The results have implications for our FCM SEA and demonstrate that the actual SLDs (Fig. 6), as expected, are not suitable to explain temporal dynamics for the entire range of soil moisture. This agrees with the findings of Takagi and Lin (2012) who stated that a soil-landform unit (SLU) is not a reasonable indicator of soil moisture spatial organization under dry conditions while different SLUs can show the same moisture content. It is clear from our analysis and others (Wilson et al., 2004) that to make a good state-space prediction of soil moisture, we need a better *a priori* stratification of the catchment from SLUs towards meaningful hydrological response units (HRUs). There is no doubt that other proxy data related to processes that control the spatial distribution of soil moisture should be included in the FCM SEA. In particular the integration of (static) soil and (dynamic) vegetation properties is an important step while they strongly affect soil moisture variation (Baggaley et al., 2009; Hu and Si, 2014). In addition, dynamic soil moisture patterns obtained from a time-lapse sequence of SAR data and cosmic-ray probes (Zreda et al., 2008) as an emerging technology may also provide useful information to further constrain the locations of HRUs in our research catchment.

Nevertheless, our proposed FCM SEA is promising for collecting data in small catchments in an efficient way to characterize and analyze temporal dynamics of soil moisture. It provides a synergistic integration of various proxy data which can be related to soil moisture. Based on a set of surrogated patterns, hydrologically relevant structures were explored with the FCM clustering technique which is a common technique in pattern recognition science. The explored patterns represent SLDs, and in a best case HRUs, which are described by fuzzy membership maps. In each SLD at least one representative sampling point is selected, and taken together they allow in combination with the fuzzy membership maps a realistic estimation of the actual soil moisture pattern. The main advantage of the FCM SEA is the small number of measurement points that form the basis to characterize and predict soil moisture patterns. Earlier studies that made measurements on regular grids like in the Tarrawarra catchment (10.5 ha, ~500 points) or that used common geostatistical techniques (such as kriging) like in the Shale Hills catchment (7.7 ha,

~189 points) need hundreds of points to obtain estimates of the spatial distribution of soil moisture (Western et al., 1998b; Lin et al., 2006). For the FCM SEA a smaller number of observation points is needed (144 ha, ~50 points) to estimate soil moisture maps. Thus, FCM SEA is a promising approach providing at least as accurate results for wet moisture states than traditional techniques but with considerably less effort. However, for the intermediate state and especially for the grassland areas the FCM SEA performance is poor and demonstrates the lack of topographic data to explain soil moisture variability. On the other hand to take more than one sample out of each cluster might be of benefit to further improve the prediction accuracy. At present only one sampling point was selected per cluster in the grassland areas and two sampling points per cluster for arable land to calibrate the FCM interpolation method. Our results show that the small scale variability of soil moisture is much higher and especially in clusters that show large within-cluster variability it is advisable to increase the number of sampling points. To test the performance of FCM SEA in a broader sense and for other sites the use of comprehensive datasets from existing networks can motivate further research to verify the estimated maps for different soil moisture states. In addition, with the FCM SEA we could suggest how to reduce the number of existing measurement points in the networks and make the observations more efficient with respect to measurement costs and maintenance effort. Nevertheless, this requires initially a very good prediction of the soil moisture maps and for the moment we first need to improve our method by adding additional variables (e.g. soil texture, land use) to reach this goal, which is an ongoing work in the Schäfertal catchment. At the moment there is still some work to be done and one should also not forget that the performance of the method might be site specific with respect to the information/attributes required to estimate good soil moisture maps. At one site, the clustering might work well with topographic data only while at other sites other properties (e.g., texture) might be responsible for driving soil moisture dynamics.

When further improved with additional variables such as soil texture and vegetation and carefully validated, such predicted maps might become useful for validation and calibration of remote sensing data (see e.g. Crow et al., 2012) and distributed models, while in future remote sensing might replace time consuming measurements. For the moment, ground based measurements are still indispensable and our proposed framework might become valuable to accompany remote sensing campaigns and modeling approaches to provide insights into the hydrological behavior of small catchments.

A priori knowledge in terms of a careful and hypothesis-driven selection of soil-moisture controlling variables is a first step to increase the sampling efficiency for soil moisture monitoring and to test the ability of the integrated data to describe the temporal dynamics of soil moisture. In a second step and based on the previously obtained results, *a posteriori* knowledge is gained and can be included in the next step by adding further proxy data that account for processes which were missing in the first step. Therefore, we see our proposed FCM SEA as a new learning framework for understanding the function of hydrological systems.

Summary and Conclusions

In this paper we applied a terrain-based FCM sampling and estimation approach (FCM SEA) to identify and characterize temporal dynamics of soil moisture in a small-scale catchment. A set of topographic attributes was selected (i.e., elevation, slope, SWI, TIR) to represent lateral flow and topographically modulated evaporative forcing. Based on this data set the FCM SEA identifies *a priori* an appropriate number of representative monitoring locations by stratifying the landscape in SLDs (unique combinations of topographic attribute values). At these points, near surface soil moisture (0-10 cm) was measured at five different sampling dates and the FCM SEA method is able to predict reasonable soil moisture patterns.

For the Schäfertal catchment results indicate that there is a transition between states characterized by a re-organization of the soil moisture pattern. During wet conditions, there is high degree of spatial organization which decreases as the soil gradually dries (intermediate conditions).

The independent validation revealed that the FCM SEA performed well and was able to explain 0.59% to 0.78% of the spatial variability of soil moisture under wet conditions, whereas under intermediate conditions its explanatory power decreased. However, the terrain-based FCM SEA was still able to account for more than 34% of the variability. Therefore, for the Schäfertal catchment, the FCM SEA is promising and superior to most studies that generally explained <50% variance.

We attribute the formation of the two distinct soil moisture patterns to a combination of several factors: (i) under wet conditions topography is the major control and drives water redistribution due to surface and subsurface lateral flow; (ii) at intermediate states the relative importance of other factors such as soil texture and vegetation become increasingly important. However, a detailed investigation of the relative contribution of these factors has not been done so far and will be part of future studies.

Acknowledgements

We would like to thank Stefan Gerlach (Agrargenossenschaft Siptenfelde) who has provided access to his fields and for his cooperation throughout this project. Assistance in field data collection was provided by Thomas Grau, Edoardo Martini, Andreas Schmidt, Martin Schrön, and Simon Kögler. We also thank Frido Reinstorf and Hermann John (University of Applied Sciences Magdeburg-Stendal) for collaboration and support, Steffen Zacharias for discussions and Hans-Jörg Vogel for comments on the manuscript. The DEM was provided with kind support of the LVermGeo LSA. We would also like to thank the two anonymous reviewers for constructive comments and suggestions which very much helped to improve the paper. This work was funded by the Helmholtz Alliance EDA – Remote Sensing and Earth System Dynamics, through the Initiative and Networking Fund of the Helmholtz Association, Germany. The research was supported by TERENO (TERrestrial ENvironmental Observatories) and by Helmholtz Impulse and Networking Fund through Helmholtz Interdisciplinary Graduate School for Environmental Research (HIGRADE) (Bissinger and Kolditz, 2008).

Figure Captions

Figure 1 Flow chart illustrating the use of the FCM cluster analysis for data/ model integration which is traditionally used for classification purposes.

Figure 2 Flow chart illustrating the FCM clustering technique used to find the adequate number of clusters for a strategic sampling and to regionally predict the target value (e.g., soil moisture).

Figure 3 Total absolute difference (TAD) for different number of clusters. Red line indicates appropriate number of clusters according to elbow method.

Figure 4 Location, topography and initial land use of the Schäfertal catchment. Meanwhile the grassland between the two roads has been transformed into arable land. Topographical data: DGM1 © GeoBasis-DE / LVermGeo LSA [2012, A13-6001119-2012]

Figure 5 Terrain attributes (a) elevation, (b) SAGA wetness index , (c) slope, and (d) annual potential incoming solar radiation derived form a 2-m DEM for the Schäfertal catchment. White lines represent creek and roads that were masked and not used in the analysis. Topographical data: DGM1 © GeoBasis-DE / LVermGeo LSA [2012, A13-6001119-2012]

Figure 6 Map of the 30 SLDs obtained with the FCM SEA.

Figure 7 Distribution of the soil moisture measurement locations. Black: Locations obtained from the FCM clustering technique (see Fig. 2) used for calibration (50 points). Red: Independent locations used for validation (44 points). White lines represent creek and roads.

Figure 8 Observed soil moisture patterns in the Schäfertal catchment for five occasions. Each dot represents the average volumetric soil moisture of three replicate TDR measurements in the top 10 cm of the soil profile.

Figure 9 Predicted maps of volumetric soil moisture content using the FCM interpolation method (Fig. 2) for different moisture states.

Figure 10 Comparison between the predicted volumetric soil moisture using the FCM interpolation method and the observed soil moisture for the five sampling dates (a-d). Horizontal bars indicate ±1 standard deviation of the observed soil moisture. (NSE: Nash-Sutcliffe coefficient of efficiency; RMSE: root mean square error)

Table 1 Main characteristics of the selected measurement campaigns in the Schäfertal

Campaign	Date	Sample Size	Soil Moisture [m^3/m^3] Mean	Median	Standard Deviation	Min	Max	Range	Antecedent Precipitation 5 Days, [mm]
T1	17/04/2013	94	0.34	0.29	0.11	0.22	0.71	0.49	15.0
T2	23/04/2013	94	0.26	0.23	0.12	0.14	0.69	0.55	0
T3	08/05/2013	94	0.27	0.24	0.09	0.16	0.69	0.53	8.8
T4	25/09/2013	94	0.19	0.17	0.07	0.12	0.48	0.36	0
T5	02/10/2013	94	0.18	0.16	0.07	0.10	0.47	0.37	0.6

Table 2 Spearman rank correlation coefficients between dates for the entire study period

Date	***17/04/2013***	***23/04/2013***	***08/05/2013***	***25/09/2013***	***02/10/2013***
Campaign	**T1**	**T2**	**T3**	**T4**	**T5**
T1	1				
T2	0.95	1			
T3	0.87	0.92	1		
T4	0.57	0.49	0.48	1	
T5	0.66	0.62	0.59	0.79	1

Table 3 Performance of the FCM SEA for the validation of arable land, grassland and the whole catchment. (NSE: Nash-Sutcliffe coefficient of efficiency; RMSE: root mean square error)

		validation for arable land		validation for grassland		validation for whole catchment (see Fig. 10)	
Campaign	Date	NSE	RMSE	NSE	RMSE	NSE	RMSE
T1	17/04/2013	0.54	0.05	0.50	0.08	0.78	0.06
T2	23/04/2013	0.52	0.04	0.37	0.10	0.73	0.06
T3	08/05/2013	0.56	0.03	0.06	0.11	0.59	0.06
T4	25/09/2013	-0.35	0.04	-0.28	0.09	0.34	0.06
T5	02/10/2013	0.28	0.03	-0.31	0.09	0.41	0.05

References

Abdank, H., Steininger, M., Altermann, M., 1995. Untersuchungen zur Landnutzung und zum Gewässerschutz im Unterharz. Mitteilungen Dtsch. Bodenkd. Ges. 77 166–173.

Albertson, J.D., Montaldo, N., 2003. Temporal dynamics of soil moisture variability: 1. Theoretical basis. Water Resour. Res. 39, 1274. doi:10.1029/2002WR001616

Altermann, M., 1985. Standortkennzeichnung landwirtschaftlich genutzter Gebiete des östlichen Harzes, Habilitationsschrift. Universität Rostock.

Applegate, D., Bixby, R., Chvátal, V., Cook, W., 2001. TSP Cuts Which Do Not Conform to the Template Paradigm, in: Jünger, M., Naddef, D. (Eds.), Computational Combinatorial Optimization, Lecture Notes in Computer Science. Springer Berlin Heidelberg, pp. 261–303.

Baggaley, N., Mayr, T., Bellamy, P., 2009. Identification of key soil and terrain properties that influence the spatial variability of soil moisture throughout the growing season. Soil Use Manag. 25, 262–273. doi:10.1111/j.1475-2743.2009.00222.x

Baroni, G., Ortuani, B., Facchi, A., Gandolfi, C., 2013. The role of vegetation and soil properties on the spatio-temporal variability of the surface soil moisture in a maize-cropped field. J. Hydrol. 489, 148–159. doi:10.1016/j.jhydrol.2013.03.007

Beaudette, D.E., Dahlgren, R.A., O'Geen, A.T., 2013. Terrain-Shape Indices for Modeling Soil Moisture Dynamics. Soil Sci. Soc. Am. J. 77, 1696–1710. doi:10.2136/sssaj2013.02.0048

Behrens, T., Zhu, A.-X., Schmidt, K., Scholten, T., 2010. Multi-scale digital terrain analysis and feature selection for digital soil mapping. Geoderma 155, 175–185. doi:10.1016/j.geoderma.2009.07.010

Beven, K.J., Kirkby, M.J., 1979. A physically based, variable contributing area model of basin hydrology / Un modèle à base physique de zone d'appel variable de l'hydrologie du bassin versant. Hydrol. Sci. Bull. 24, 43–69. doi:10.1080/02626667909491834

Bezdek, D.J.C., 1974. Numerical taxonomy with fuzzy sets. J. Math. Biol. 1, 57–71. doi:10.1007/BF02339490

Bezdek, J.C., Ehrlich, R., Full, W., 1984. FCM: The fuzzy c-means clustering algorithm. Comput. Geosci. 10, 191–203. doi:10.1016/0098-3004(84)90020-7

Bissinger, V., Kolditz, O., 2008. Helmholtz Interdisciplinary Graduate School for Environmental Research (HIGRADE) GAIA 1(2008):71–73.

Bogena, H.R., Herbst, M., Huisman, J.A., Rosenbaum, U., Weuthen, A., Vereecken, H., 2010. Potential of Wireless Sensor Networks for Measuring Soil Water Content Variability. Vadose Zone J. 9, 1002–1013. doi:10.2136/vzj2009.0173

Böhner, J., Selige, T., 2006. Spatial prediction of soil attributes using terrain analysis and climate regionalisation, in: Böhner, J., McCloy, K.R., Strobl, J. (Eds.), SAGA–Analyses and Modelling Applications. Göttinger Geographische Abhandlungen, Göttingen, pp. 13–28.

Borchardt, D., 1982. Geoökologische Erkundung und hydrologische Analyse von Kleineinzugsgebieten des unteren Mittelgebirgsbereiches, dargestellt am Beispiel von Experimentalgebieten der oberen Selke/Harz. Petermanns Geogr. Mitteilungen 482 251–262.

Bronstert, A., Creutzfeldt, B., Graeff, T., Hajnsek, I., Heistermann, M., Itzerott, S., Jagdhuber, T., Kneis, D., Lück, E., Reusser, D., Zehe, E., 2012. Potentials and constraints of different types of soil moisture observations for flood simulations in headwater catchments. Nat. Hazards 60, 879–914. doi:10.1007/s11069-011-9874-9

Burrough, P.A., van Gaans, P.F.M., MacMillan, R.A., 2000. High-resolution landform classification using fuzzy k-means. Fuzzy Sets Syst. 113, 37–52. doi:10.1016/S0165-0114(99)00011-1

Cardell-Oliver, R., Kranz, M., Smettem, K., Mayer, K., 2005. A Reactive Soil Moisture Sensor Network: Design and Field Evaluation. Int. J. Distrib. Sens. Netw. 1, 149–162. doi:10.1080/15501320590966422

Crow, W.T., Berg, A.A., Cosh, M.H., Loew, A., Mohanty, B.P., Panciera, R., de Rosnay, P., Ryu, D., Walker, J.P., 2012. Upscaling sparse ground-based soil moisture observations for the validation of coarse-resolution satellite soil moisture products. Rev. Geophys. 50, RG2002. doi:10.1029/2011RG000372

De Gruijter, J.J., Brus, D., Bierkens, M., Knotters, M., 2006. Sampling for natural resource monitoring. Springer, Berlin.

Famiglietti, J.S., Rudnicki, J.W., Rodell, M., 1998. Variability in surface moisture content along a hillslope transect: Rattlesnake Hill, Texas. J. Hydrol. 210, 259–281. doi:10.1016/S0022-1694(98)00187-5

Grayson, R.B., Blöschl, G., Western, A.W., McMahon, T.A., 2002. Advances in the use of observed spatial patterns of catchment hydrological response. Adv. Water Resour. 25, 1313–1334. doi:10.1016/S0309-1708(02)00060-X

Grayson, R.B., Western, A.W., 1998. Towards areal estimation of soil water content from point measurements: time and space stability of mean response. J. Hydrol. 207, 68–82. doi:10.1016/S0022-1694(98)00096-1

Grayson, R.B., Western, A.W., Chiew, F.H.S., Blöschl, G., 1997. Preferred states in spatial soil moisture patterns: Local and nonlocal controls. Water Resour. Res. 33, 2897–2908. doi:10.1029/97WR02174

Hachmöller, B., Paasche, H., 2013. Integration of surface-based tomographic models for zonation and multimodel guided extrapolation of sparsely known petrophysical parameters. GEOPHYSICS 78, EN43–EN53. doi:10.1190/geo2012-0417.1
Hudson, B.D., 1992. The Soil Survey as Paradigm-based Science. Soil Sci. Soc. Am. J. 56, 836. doi:10.2136/sssaj1992.03615995005600030027x
Hupet, F., Vanclooster, M., 2002. Intraseasonal dynamics of soil moisture variability within a small agricultural maize cropped field. J. Hydrol. 261, 86–101. doi:10.1016/S0022-1694(02)00016-1
Hu, W., Si, B.C., 2014a. Revealing the relative influence of soil and topographic properties on soil water content distribution at the watershed scale in two sites. J. Hydrol., Determination of soil moisture: Measurements and theoretical approaches 516, 107–118. doi:10.1016/j.jhydrol.2013.10.002
Hu, W., Si, B.C., 2014b. Revealing the relative influence of soil and topographic properties on soil water content distribution at the watershed scale in two sites. J. Hydrol., Determination of soil moisture: Measurements and theoretical approaches 516, 107–118. doi:10.1016/j.jhydrol.2013.10.002
Jenny, H., 1941. Factors of Soil Formation: A System of Quantitative Pedology. McGraw-Hill Book Co., New York.
Kachanoski, R.G., de Jong, E., 1988. Scale dependence and the temporal persistence of spatial patterns of soil water storage. Water Resour. Res. 24, 85–91. doi:10.1029/WR024i001p00085
Lassonde, M., 2001. Approximation, Optimization and Mathematical Economics, Softcover reprint of the original 1st ed. 2001. ed. Physica.
Leekwijck, W.V., Kerre, E.E., 1999. Defuzzification: criteria and classification. Fuzzy Sets Syst. 108, 159–178. doi:10.1016/S0165-0114(97)00337-0
Lesch, S.M., 2005. Sensor-directed response surface sampling designs for characterizing spatial variation in soil properties. Comput. Electron. Agric., Applications of Apparent Soil Electrical Conductivity in Precision Agriculture 46, 153–179. doi:10.1016/j.compag.2004.11.004
Lin, H., 2003. Hydropedology Bridging Disciplines, Scales, and Data. Vadose Zone J. 2, 1–11. doi:10.2113/2.1.1
Lin, H.S., Kogelmann, W., Walker, C., Bruns, M.A., 2006. Soil moisture patterns in a forested catchment: A hydropedological perspective. Geoderma 131, 345–368. doi:10.1016/j.geoderma.2005.03.013
MacMillan, R.A., Pettapiece, W.W., Nolan, S.C., Goddard, T.W., 2000. A generic procedure for automatically segmenting landforms into landform elements using DEMs, heuristic rules and fuzzy logic. Fuzzy Sets Syst. 113, 81–109. doi:10.1016/S0165-0114(99)00014-7
Martinez, C., Hancock, G.R., Kalma, J.D., Wells, T., 2008. Spatio-temporal distribution of near-surface and root zone soil moisture at the catchment scale. Hydrol. Process. 22, 2699–2714. doi:10.1002/hyp.6869
Martínez-Fernández, J., Ceballos, A., 2005. Mean soil moisture estimation using temporal stability analysis. J. Hydrol. 312, 28–38. doi:10.1016/j.jhydrol.2005.02.007
Martini, E., Wollschläger, U., Kögler, S., Behrens, T., Dietrich, P., Reinstorf, F., Schmidt, K., Weiler, M., Werban, U., Zacharias, S., 2015. Spatial and Temporal Dynamics of

Hillslope-Scale Soil Moisture Patterns: Characteristic States and Transition Mechanisms. Vadose Zone J. 0, 0. doi:10.2136/vzj2014.10.0150

McBratney, A.B., Santos, M.L.M., Minasny, B., 2003. On digital soil mapping. Geoderma 117, 3–52. doi:10.1016/S0016-7061(03)00223-4

McKenzie, N.J., Ryan, P.J., 1999. Spatial prediction of soil properties using environmental correlation. Geoderma 89, 67–94. doi:10.1016/S0016-7061(98)00137-2

Merz, B., Plate, E.J., 1997. An analysis of the effects of spatial variability of soil and soil moisture on runoff. Water Resour. Res. 33, 2909–2922. doi:10.1029/97WR02204

Meyer, D., Dimitriadou, E., Hornik, K., Weingessel, A., Leisch, F., [C++-code - Chih-Chung Chang (libsvm)], [C++-code - Chih-Chen Lin (libsvm)], 2014. e1071: Misc Functions of the Department of Statistics (e1071), TU Wien, R package version 1.6-1 <http://cran.r-project.org/package=e1071 (Accessed February 10, 2013).

Minasny, B., McBratney, A.B., 2006. A conditioned Latin hypercube method for sampling in the presence of ancillary information. Comput. Geosci. 32, 1378–1388. doi:10.1016/j.cageo.2005.12.009

Moore, I.D., Grayson, R.B., Ladson, A.R., 1991. Digital terrain modelling: A review of hydrological, geomorphological, and biological applications. Hydrol. Process. 5, 3–30. doi:10.1002/hyp.3360050103

Nash, J.E., Sutcliffe, J.V., 1970. River flow forecasting through conceptual models part I — A discussion of principles. J. Hydrol. 10, 282–290. doi:10.1016/0022-1694(70)90255-6

Odeh, I.O.A., Chittleborough, D.J., McBratney, A.B., 1992. Soil Pattern Recognition with Fuzzy-c-means: Application to Classification and Soil-Landform Interrelationships. Soil Sci. Soc. Am. J. 56, 505. doi:10.2136/sssaj1992.03615995005600020027x

Odeh, I.O.A., McBratney, A.B., Chittleborough, D.J., 1990. Design of optimal sample spacings for mapping soil using fuzzy-k-means and regionalized variable theory. Geoderma 47, 93–122. doi:10.1016/0016-7061(90)90049-F

Ollesch, G., Kistner, I., Meissner, R., Lindenschmidt, K.-E., 2006. Modelling of snowmelt erosion and sediment yield in a small low-mountain catchment in Germany. CATENA 68, 161–176. doi:10.1016/j.catena.2006.04.005

Paasche, H., Eberle, D.G., 2009. Rapid integration of large airborne geophysical data suites using a fuzzy partitioning cluster algorithm: a tool for geological mapping and mineral exploration targeting. Explor. Geophys. 40, 277–287.

Paasche, H., Tronicke, J., Holliger, K., Green, A.G., Maurer, H., 2006. Integration of diverse physical-property models: Subsurface zonation and petrophysical parameter estimation based on fuzzy c-means cluster analyses. Geophysics 71, H33–H44. doi:10.1190/1.2192927

Penna, D., Borga, M., Norbiato, D., Dalla Fontana, G., 2009. Hillslope scale soil moisture variability in a steep alpine terrain. J. Hydrol. 364, 311–327. doi:10.1016/j.jhydrol.2008.11.009

Qu, W., Bogena, H.R., Huisman, J.A., Vanderborght, J., Schuh, M., Priesack, E., Vereecken, H., 2015. Predicting subgrid variability of soil water content from basic soil information. Geophys. Res. Lett. 42, 2014GL062496. doi:10.1002/2014GL062496

R Development Core Team, 2012. R: A language and environment for statistical computing. R Foundation for Statistical Computing, Vienna, Austria. ISBN 3-900051-07-0 <http://www.R-project.org> (Accessed August 15, 2012).

Reinstorf, F., 2010. Schäfertal, Harz Mountains, Germany. Poster. In: Schumann, S., B. Schmalz, H. Meesenburg, and U. Schröder (Eds.), “Status and Perspectives of Hydrology in Small Basins”, Results and reccommendations of the International Workshop in Goslar-Hahnenklee, Germany 2009, and Inventory of Small Hydrological Research Basin. 30 March – 2 April 2009, Goslar-Hahnenklee, Germany.

Robinson, D.A., Campbell, C.S., Hopmans, J.W., Hornbuckle, B.K., Jones, S.B., Knight, R., Ogden, F., Selker, J., Wendroth, O., 2008. Soil Moisture Measurement for Ecological and Hydrological Watershed-Scale Observatories: A Review. Vadose Zone J. 7, 358. doi:10.2136/vzj2007.0143

Rosenbaum, U., Bogena, H.R., Herbst, M., Huisman, J.A., Peterson, T.J., Weuthen, A., Western, A.W., Vereecken, H., 2012. Seasonal and event dynamics of spatial soil moisture patterns at the small catchment scale. Water Resour. Res. 48, n/a–n/a. doi:10.1029/2011WR011518

Roth, K., Schulin, R., Flühler, H., Attinger, W., 1990. Calibration of time domain reflectometry for water content measurement using a composite dielectric approach. Water Resour. Res. 26, 2267–2273. doi:10.1029/WR026i010p02267

Roubens, M., 1982. Fuzzy clustering algorithms and their cluster validity. Eur. J. Oper. Res. 10, 294–301. doi:10.1016/0377-2217(82)90228-4

Schmidt, K., Behrens, T., Daumann, J., Ramirez-Lopez, L., Werban, U., Dietrich, P., Scholten, T., 2014. A comparison of calibration sampling schemes at the field scale. Geoderma 232–234, 243–256. doi:10.1016/j.geoderma.2014.05.013

Schneider, K., Huisman, J.A., Breuer, L., Zhao, Y., Frede, H.-G., 2008. Temporal stability of soil moisture in various semi-arid steppe ecosystems and its application in remote sensing. J. Hydrol. 359, 16–29. doi:10.1016/j.jhydrol.2008.06.016

Schulz, K., Seppelt, R., Zehe, E., Vogel, H.J., Attinger, S., 2006. Importance of spatial structures in advancing hydrological sciences. Water Resour. Res. 42, W03S03. doi:10.1029/2005WR004301

Soulsby, C., Neal, C., Laudon, H., Burns, D.A., Merot, P., Bonell, M., Dunn, S.M., Tetzlaff, D., 2008. Catchment data for process conceptualization: simply not enough? Hydrol. Process. 22, 2057–2061. doi:10.1002/hyp.7068

Stevenson, B.A., McNeill, S., Hewitt, A.E., 2015. Characterising soil quality clusters in relation to land use and soil order in New Zealand: An application of the phenoform concept. Geoderma 239–240, 135–142. doi:10.1016/j.geoderma.2014.10.003

Sun, X.-L., Zhao, Y.-G., Wang, H.-L., Yang, L., Qin, C.-Z., Zhu, A.-X., Zhang, G.-L., Pei, T., Li, B.-L., 2012. Sensitivity of digital soil maps based on FCM to the fuzzy exponent and the number of clusters. Geoderma, Entering the Digital Era: Special Issue of Pedometrics 2009, Beijing 171–172, 24–34. doi:10.1016/j.geoderma.2011.03.016

Takagi, K., Lin, H.S., 2012. Changing controls of soil moisture spatial organization in the Shale Hills Catchment. Geoderma 173–174, 289–302. doi:10.1016/j.geoderma.2011.11.003

Triantafilis, J., Gibbs, I., Earl, N., 2013. Digital soil pattern recognition in the lower Namoi valley using numerical clustering of gamma-ray spectrometry data. Geoderma 192, 407–421. doi:10.1016/j.geoderma.2012.08.021

Triantafilis, J., Odeh, I.O.A., Minasny, B., McBratney, A.B., 2003. Elucidation of physiographic and hydrogeological features of the lower Namoi valley using fuzzy k-means classification of EM34 data. Environ. Model. Softw. 18, 667–680. doi:10.1016/S1364-8152(03)00053-7

Twarakavi, N.K.C., Šimůnek, J., Schaap, M.G., 2010. Can texture-based classification optimally classify soils with respect to soil hydraulics? Water Resour. Res. 46, W01501. doi:10.1029/2009WR007939

Vachaud, G., Passerat De Silans, A., Balabanis, P., Vauclin, M., 1985. Temporal Stability of Spatially Measured Soil Water Probability Density Function. Soil Sci. Soc. Am. J. 49, 822. doi:10.2136/sssaj1985.03615995004900040006x

Van Arkel, Z., Kaleita, A.L., 2014. Identifying sampling locations for field-scale soil moisture estimation using K-means clustering. Water Resour. Res. 50, 7050–7057. doi:10.1002/2013WR015015

Vereecken, H., Huisman, J.A., Pachepsky, Y., Montzka, C., van der Kruk, J., Bogena, H., Weihermüller, L., Herbst, M., Martinez, G., Vanderborght, J., 2014. On the spatio-temporal dynamics of soil moisture at the field scale. J. Hydrol., Determination of soil moisture: Measurements and theoretical approaches 516, 76–96. doi:10.1016/j.jhydrol.2013.11.061

Wagner, W., Bloeschl, G., Pampaloni, P., Calvet, J.-C., Bizzarri, B., Wigneron, J.-P., Kerr, Y., 2007. Operational readiness of microwave remote sensing of soil moisture for hydrologic applications. Nord. Hydrol. 38, 1–20. doi:10.2166/nh.2007.029

Werbylo, K.L., Niemann, J.D., 2014. Evaluation of sampling techniques to characterize topographically-dependent variability for soil moisture downscaling. J. Hydrol., Determination of soil moisture: Measurements and theoretical approaches 516, 304–316. doi:10.1016/j.jhydrol.2014.01.030

Western, A., Grayson, R., 2000. Soil moisture and runoff processes at Tarrawarra. In: Grayson, R.; Blöschl G. (Eds.), Spatial Patterns in Catchment Hydrology Observations and Modelling. Cambridge: Cambridge University Press; 2000. p. 209–246 [chapter 9].

Western, A.W., Blöschl, G., Grayson, R.B., 1998. Geostatistical characterisation of soil moisture patterns in the Tarrawarra catchment. J. Hydrol. 205, 20–37. doi:10.1016/S0022-1694(97)00142-X

Western, A.W., Grayson, R.B., 1998. The Tarrawarra Data Set: Soil moisture patterns, soil characteristics, and hydrological flux measurements. Water Resour. Res. 34, 2765–2768. doi:10.1029/98WR01833

Western, A.W., Grayson, R.B., Blöschl, G., Willgoose, G.R., McMahon, T.A., 1999a. Observed spatial organization of soil moisture and its relation to terrain indices. Water Resour. Res. 35, 797–810. doi:10.1029/1998WR900065

Western, A.W., Grayson, R.B., Blöschl, G., Willgoose, G.R., McMahon, T.A., 1999b. Observed spatial organization of soil moisture and its relation to terrain indices. Water Resour. Res. 35, 797–810. doi:10.1029/1998WR900065

Western, A.W., Grayson, R.B., Green, T.R., 1999c. The Tarrawarra project: high resolution spatial measurement, modelling and analysis of soil moisture and hydrological response. Hydrol. Process. 13, 633–652. doi:10.1002/(SICI)1099-1085(19990415)13:5<633::AID-HYP770>3.0.CO;2-8

Western, A.W., Zhou, S.-L., Grayson, R.B., McMahon, T.A., Blöschl, G., Wilson, D.J., 2004. Spatial correlation of soil moisture in small catchments and its relationship to dominant spatial hydrological processes. J. Hydrol. 286, 113–134. doi:10.1016/j.jhydrol.2003.09.014

Wilson, D.J., Western, A.W., Grayson, R.B., 2005. A terrain and data-based method for generating the spatial distribution of soil moisture. Adv. Water Resour. 28, 43–54. doi:10.1016/j.advwatres.2004.09.007

Wilson, D.J., Western, A.W., Grayson, R.B., 2004. Identifying and quantifying sources of variability in temporal and spatial soil moisture observations. Water Resour. Res. 40, W02507. doi:10.1029/2003WR002306

Wilson, D.J., Western, A.W., Grayson, R.B., Berg, A.A., Lear, M.S., Rodell, M., Famiglietti, J.S., Woods, R.A., McMahon, T.A., 2003. Spatial distribution of soil moisture over 6 and 30 cm depth, Mahurangi river catchment, New Zealand. J. Hydrol. 276, 254–274. doi:10.1016/S0022-1694(03)00060-X

Wilson, J.P., Gallant, J.C., 2000. Terrain Analysis: Principles and Applications. John Wiley & Sons, New York [etc.].

Woods, R., Grayson, R., Western, A., Duncan, M., Wilson, D., Young, R., Ibbitt, R., Henderson, R., McMahon, T., 2001. Experimental Design and Initial Results from the Mahurangi River Variability Experiment: MARVEX, in: Lakshmi, V., Albertson, J., Schaake, J. (Eds.), Land Surface Hydrology, Meteorology, and Climate: Observations and Modeling. American Geophysical Union, pp. 201–213.

Zacharias, S., Bogena, H., Samaniego, L., Mauder, M., Fuß, R., Pütz, T., Frenzel, M., Schwank, M., Baessler, C., Butterbach-Bahl, K., Bens, O., Borg, E., Brauer, A., Dietrich, P., Hajnsek, I., Helle, G., Kiese, R., Kunstmann, H., Klotz, S., Munch, J.C., Papen, H., Priesack, E., Schmid, H.P., Steinbrecher, R., Rosenbaum, U., Teutsch, G., Vereecken, H., 2011. A Network of Terrestrial Environmental Observatories in Germany. Vadose Zone J. 10, 955–973. doi:10.2136/vzj2010.0139

Zreda, M., Desilets, D., Ferré, T.P.A., Scott, R.L., 2008. Measuring soil moisture content non-invasively at intermediate spatial scale using cosmic-ray neutrons. Geophys. Res. Lett. 35, L21402. doi:10.1029/2008GL035655

Zucco, G., Brocca, L., Moramarco, T., Morbidelli, R., 2014. Influence of land use on soil moisture spatial–temporal variability and monitoring. J. Hydrol., Determination of soil moisture: Measurements and theoretical approaches 516, 193–199. doi:10.1016/j.jhydrol.2014.01.043

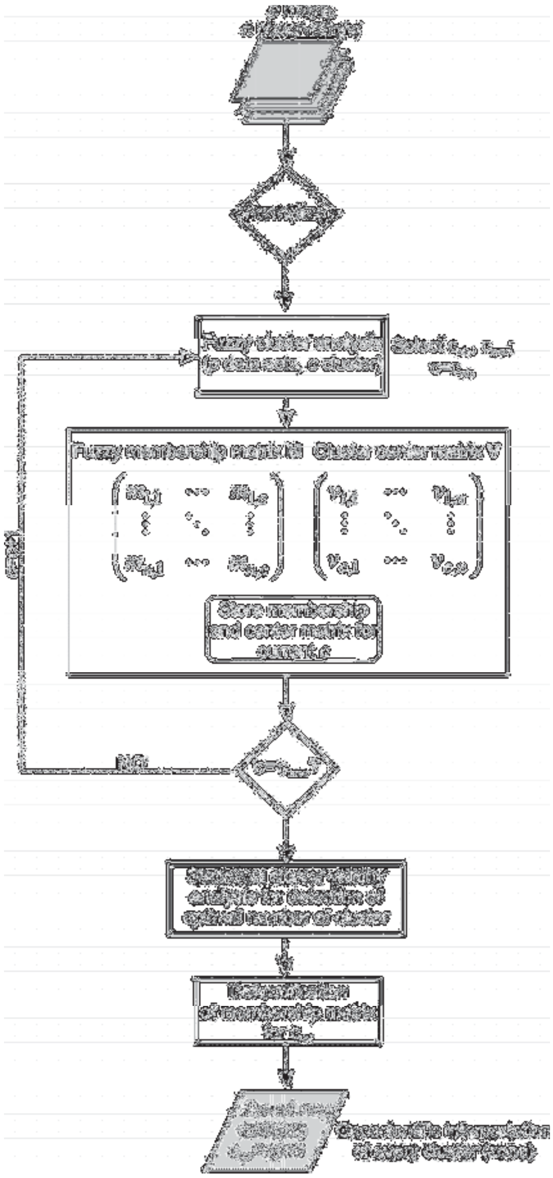

Flow chart illustrating the use of the FCM cluster analysis for data/ model integration which is traditionally used for classification purposes.
84x181mm (300 x 300 DPI)

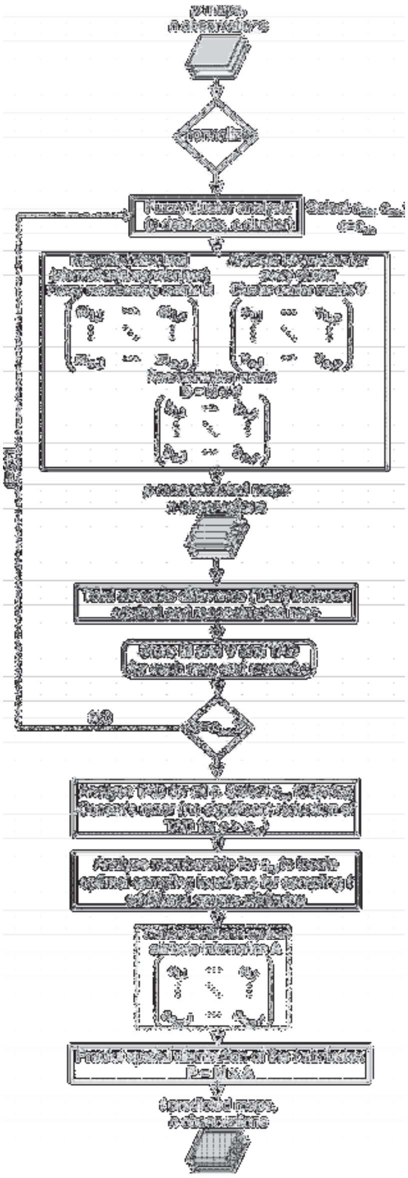

Flow chart illustrating the FCM clustering technique used to find the adequate number of clusters for a strategic sampling and to regionally predict the target value (e.g., soil moisture).
75x220mm (300 x 300 DPI)

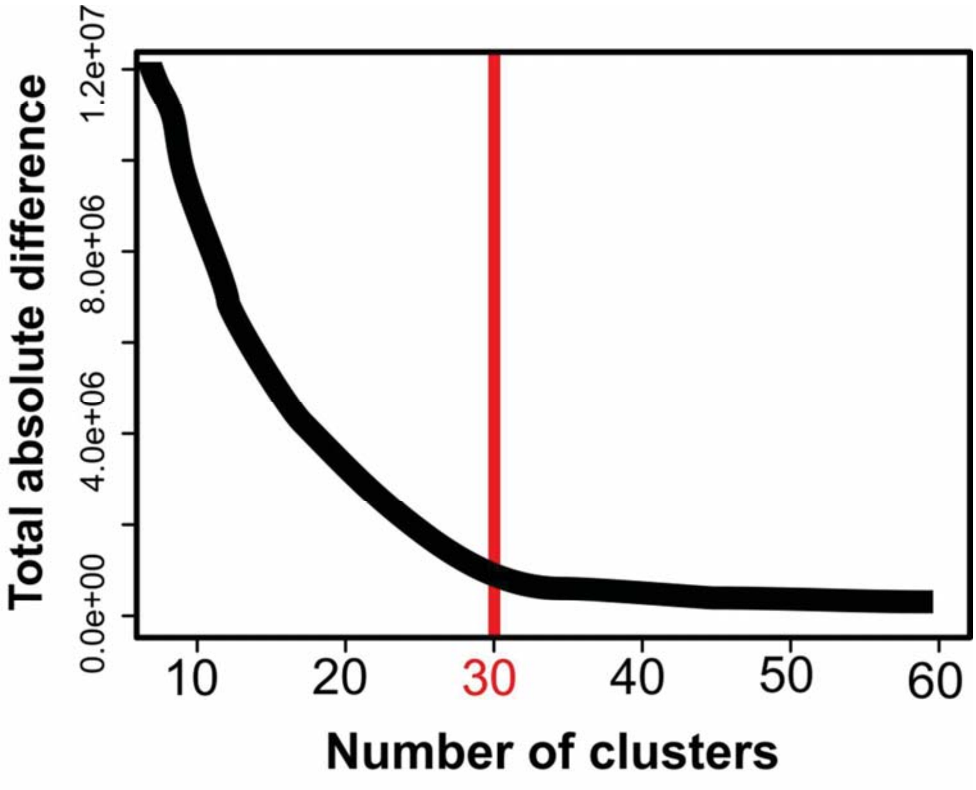

Total absolute difference (TAD) for different number of clusters. Red line indicates appropriate number of clusters according to elbow method.
82x67mm (300 x 300 DPI)

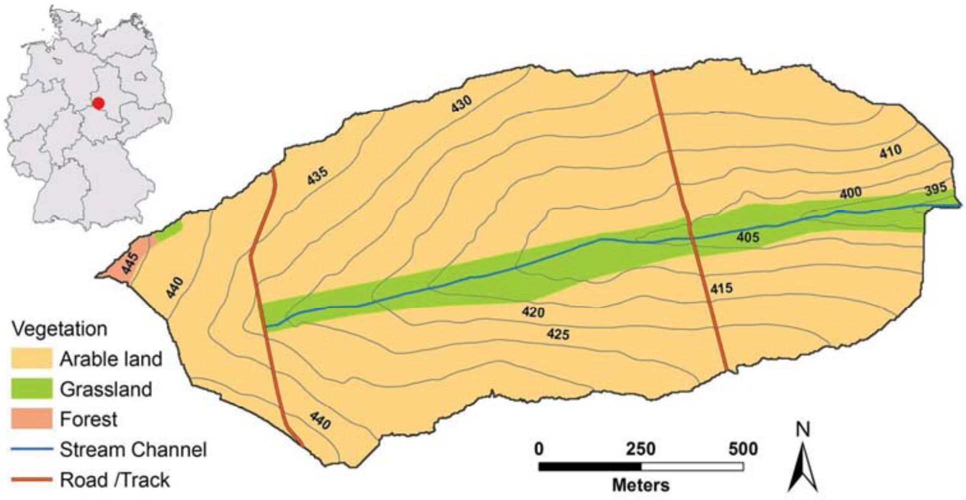

Location, topography and initial land use of the Schäfertal catchment. Meanwhile the grassland between the two roads has been transformed into arable land. Topographical data: DGM1 © GeoBasis-DE / LVermGeo LSA [2012, A13-6001119-2012]
209x148mm (300 x 300 DPI)

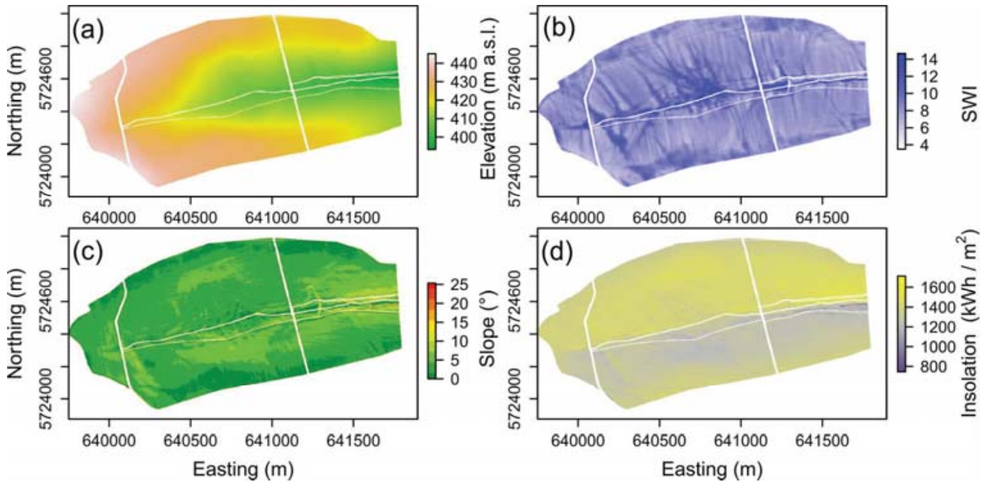

Terrain attributes (a) elevation, (b) SAGA wetness index , (c) slope, and (d) annual potential incoming solar radiation derived form a 2-m DEM for the Schäfertal catchment. White lines represent creek and roads that were masked and not used in the analysis. Topographical data: DGM1 © GeoBasis-DE / LVermGeo LSA [2012, A13-6001119-2012]
180x88mm (300 x 300 DPI)

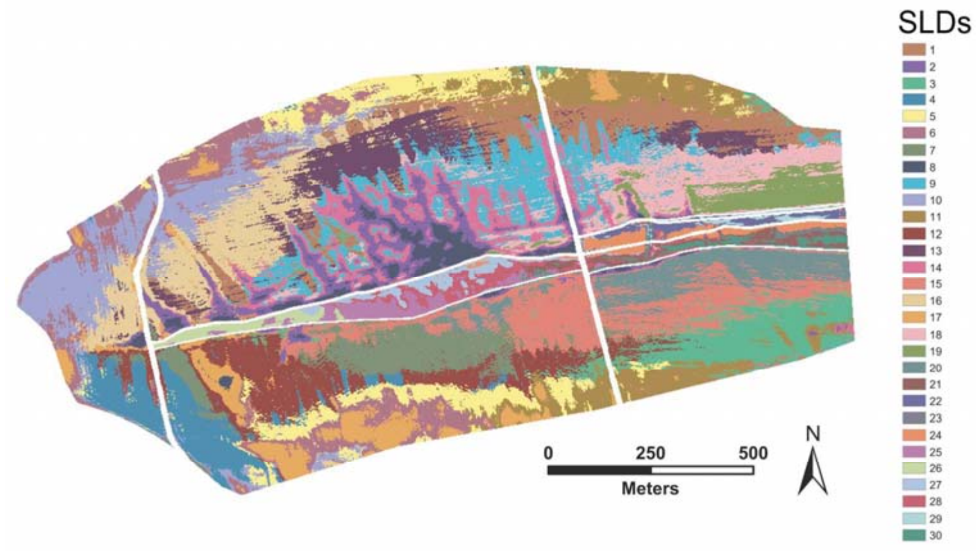

Map of the 30 SLDs obtained with the FCM SEA.
159x90mm (300 x 300 DPI)

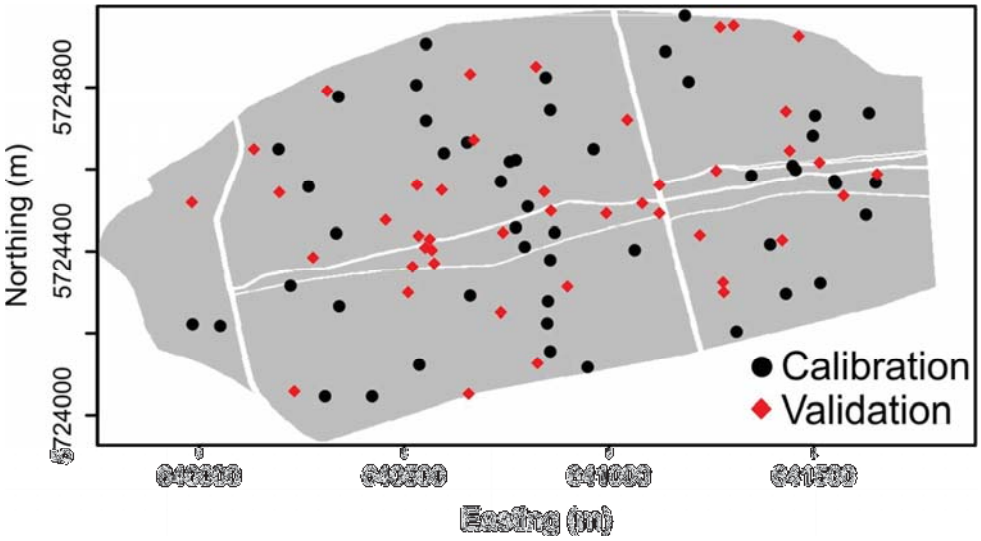

Distribution of the soil moisture measurement locations. Black: Locations obtained from the FCM clustering technique (see Fig. 2) used for calibration (50 points). Red: Independent locations used for validation (44 points). White lines represent creek and roads.
86x47mm (300 x 300 DPI)

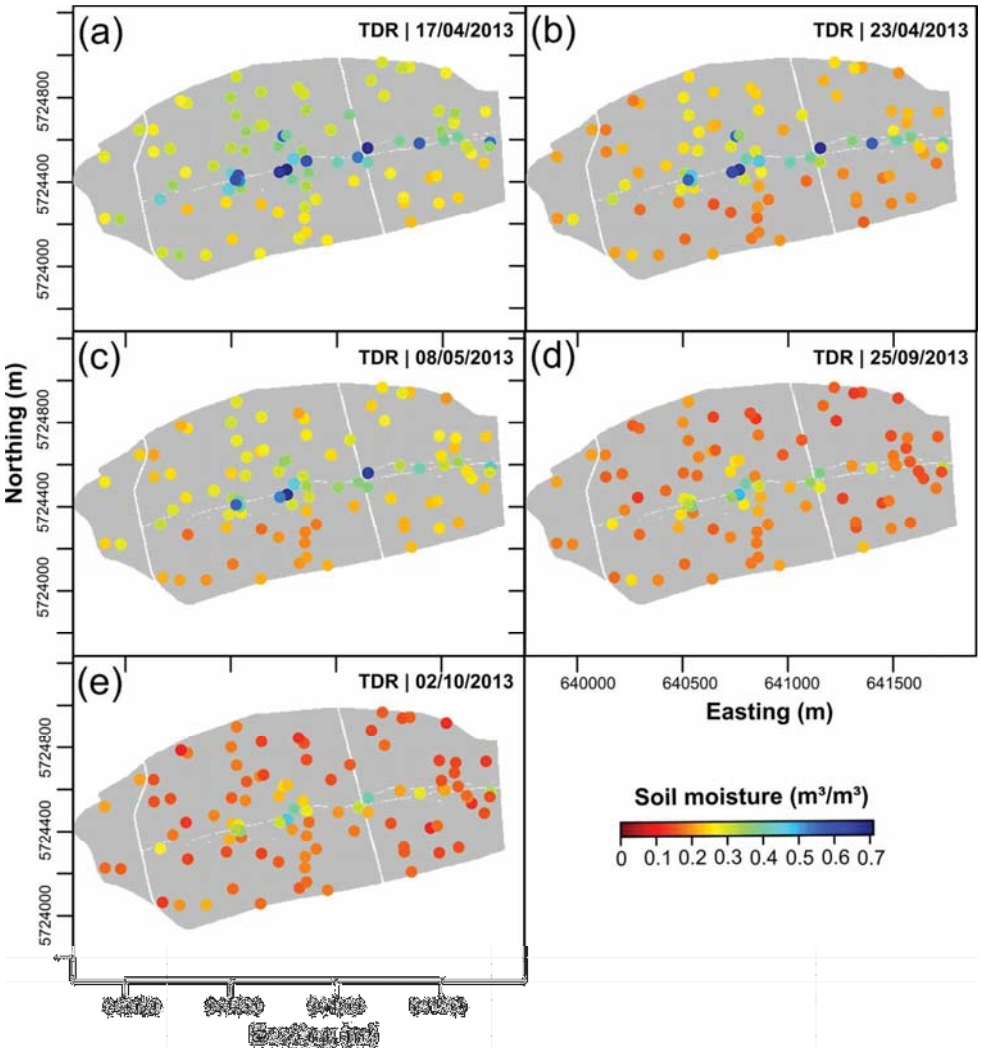

Observed soil moisture patterns in the Schäfertal catchment for five occasions. Each dot represents the average volumetric soil moisture of three replicate TDR measurements in the top 10 cm of the soil profile.
128x138mm (300 x 300 DPI)

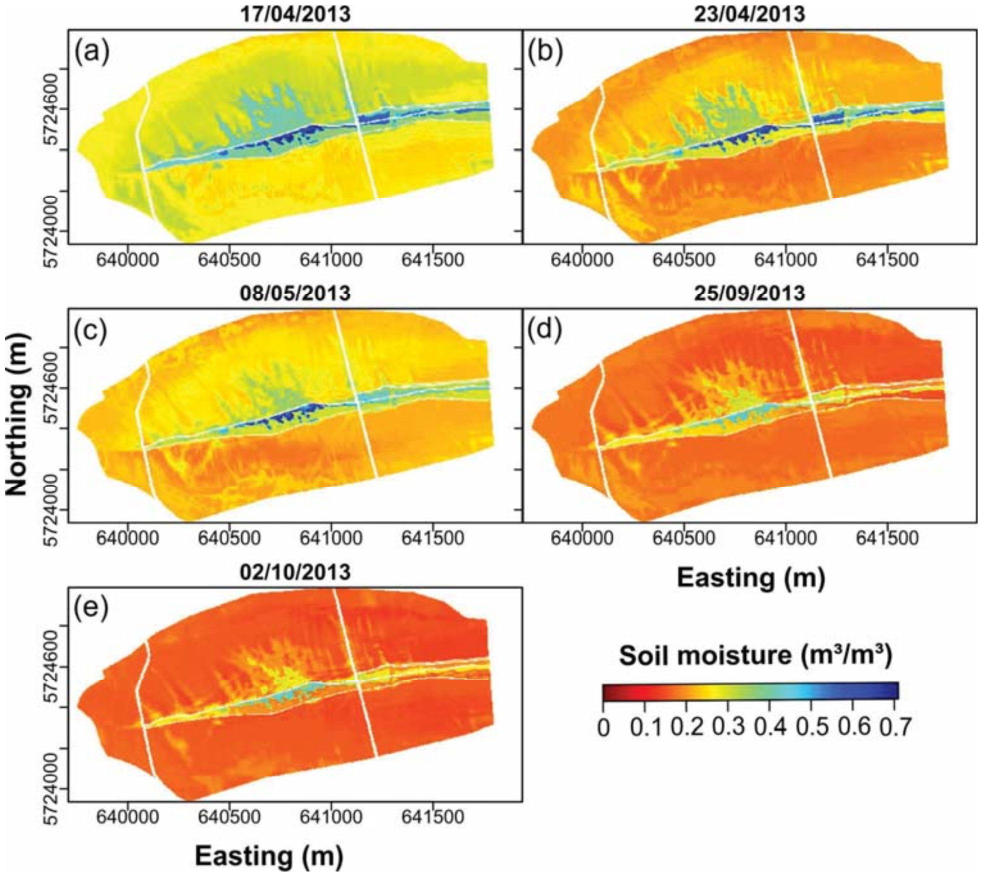

Predicted maps of volumetric soil moisture content using the FCM interpolation method (Fig. 2) for different moisture states.
164x146mm (300 x 300 DPI)

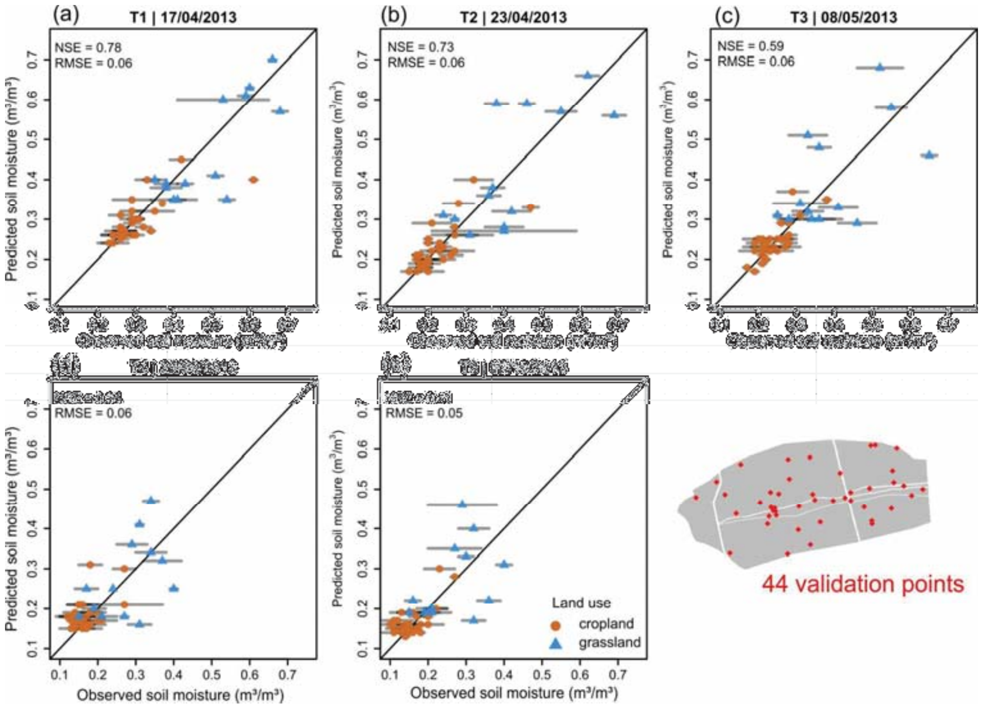

Comparison between the predicted volumetric soil moisture using the FCM interpolation method and the observed soil moisture for the five sampling dates (a-d). Horizontal bars indicate "±1" standard deviation of the observed soil moisture. (NSE: Nash-Sutcliffe coefficient of efficiency; RMSE: root mean square error)
160x115mm (300 x 300 DPI)

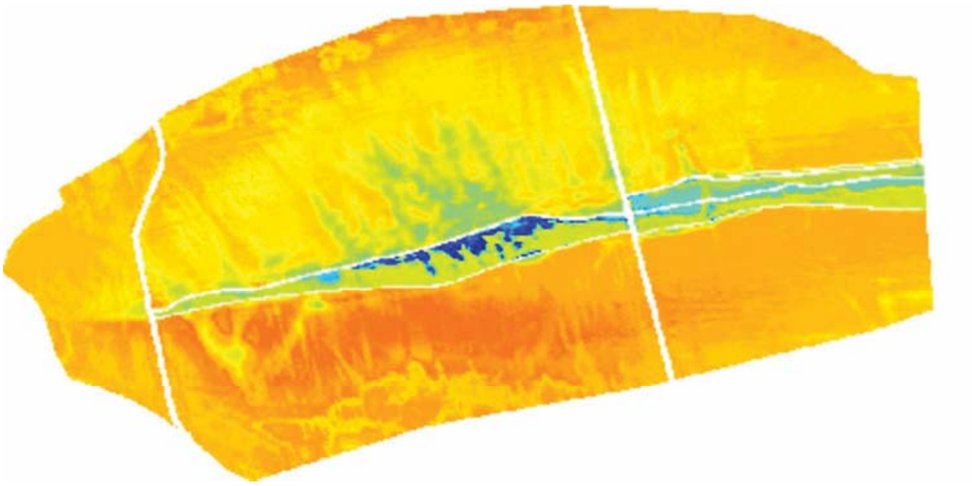

Cover
94x46mm (300 x 300 DPI)